Original Article

MOLECULAR METABOLISM

Adaptive gene expression of alternative splicing variants of PGC-1α regulates whole-body energy metabolism

Kazuhiro Nomura[1,2,3], Shinichi Kinoshita[1], Nao Mizusaki[1], Yoko Senga[1], Tsutomu Sasaki[4], Tadahiro Kitamura[5], Hiroshi Sakaue[2,6], Aki Emi[1], Tetsuya Hosooka[1,7], Masahiro Matsuo[8], Hitoshi Okamura[8,9], Taku Amo[10], Alexander M. Wolf[11], Naomi Kamimura[11,12], Shigeo Ohta[11], Tomoo Itoh[13], Yoshitake Hayashi[13], Hiroshi Kiyonari[14], Anna Krook[3], Juleen R. Zierath[3], Masato Kasuga[15], Wataru Ogawa[1,*]

ABSTRACT

The transcriptional coactivator PGC-1α has been implicated in the regulation of multiple metabolic processes. However, the previously reported metabolic phenotypes of mice deficient in PGC-1α have been inconsistent. PGC-1α exists as multiple isoforms, including variants transcribed from an alternative first exon. We show here that alternative PGC-1α variants are the main entity that increases PGC-1α during exercise. These variants, unlike the canonical isoform of PGC-1α, are robustly upregulated in human skeletal muscle after exercise. Furthermore, the extent of this upregulation correlates with oxygen consumption. Mice lacking these variants manifest impaired energy expenditure during exercise, leading to the development of obesity and hyperinsulinemia. The alternative variants are also upregulated in brown adipose tissue in response to cold exposure, and mice lacking these variants are intolerant of a cold environment. Our findings thus indicate that an increase in PGC-1α expression, attributable mostly to upregulation of alternative variants, is pivotal for adaptive enhancement of energy expenditure and heat production and thereby essential for the regulation of whole-body energy metabolism.

Keywords PGC-1α; Skeletal muscle; Exercise; Obesity; Diabetes; Energy expenditure

1. INTRODUCTION

Peroxisome proliferator-activated receptor γ (PPARγ) coactivator-1α (PGC-1α) is a transcriptional coactivator that regulates various metabolic processes including mitochondrial biogenesis, maintenance of energy homeostasis, and thermogenesis [1]. Mitochondrial dysfunction as well as impaired energy metabolism and thermogenesis are often observed in individuals with insulin resistance and obesity [2], and the abundance of PGC-1α is reduced in skeletal muscle of animals and humans with these conditions [3—6]. Impaired function of PGC-1α has therefore been implicated in the pathogenesis of these global health problems.

In spite of the large body of clinical and biochemical evidence supporting such a role for PGC-1α [1,2], the phenotypes of mice in which the PGC-1α gene has been manipulated have manifested seemingly inconsistent phenotypes. Although some lines of transgenic mice overexpressing PGC-1α exhibit phenotypes characterized by obesity resistance or insulin sensitivity [7,8], others do not, with some manifesting insulin resistance or glucose intolerance under certain conditions [9—11]. Mice lacking the PGC-1α gene have also not clarified the contribution of this protein to insulin resistance or obesity. Mice with whole-body PGC-1α deficiency are paradoxically insulin sensitive rather than insulin resistant, with a reduced body mass or a slightly increased body mass only in aged females [12,13]. Muscle-specific PGC-1α-deficient mice are also insulin sensitive and have a normal body mass [14]. Although mice lacking PGC-1α specifically in adipocytes manifest impaired insulin sensitivity when fed a high-fat diet, their body mass does not differ from that of control animals when fed either a high-fat or normal diet [15].

[1]Division of Diabetes and Endocrinology, Department of Internal Medicine, Kobe University Graduate School of Medicine, Kobe 650-0017, Japan [2]Department of Nutrition and Metabolism, Institute of Biomedical Sciences, Tokushima University Graduate School, Tokushima 770-8503, Japan [3]Department of Physiology and Pharmacology, Karolinska Institutet, Stockholm 17177, Sweden [4]Division of Food Science and Biotechnology, Graduate School of Agriculture, Kyoto University, Kyoto 606-8502, Japan [5]Metabolic Signal Research Center, Institute for Molecular and Cellular Regulation, Gunma University, Maebashi 371-8512, Japan [6]Diabetes Therapeutics and Research Center, University of Tokushima, Tokushima 770-8503, Japan [7]Laboratory of Nutritional Physiology, Graduate School of Integrated Pharmaceutical and Nutritional Sciences, University of Shizuoka, Shizuoka 422-8526, Japan [8]Department of Systems Biology, Graduate School of Pharmaceutical Sciences, Kyoto University, Kyoto 606-8501, Japan [9]Department of Neuroscience, Graduate School of Medicine, Kyoto University, Kyoto 606-8303, Japan [10]Department of Applied Chemistry, National Defense Academy, Yokosuka 239-8686, Japan [11]Department of Biochemistry and Cell Biology, Graduate School of Medicine, Nippon Medical School, Kawasaki 211-8533, Japan [12]Laboratory for Clinical Research, Collaborative Research Center, Nippon Medical School, Tokyo 113-8602, Japan [13]Department of Pathology, Kobe University Graduate School of Medicine, Kobe 650-0017, Japan [14]Laboratory for Animal Resources and Genetic Engineering, RIKEN Center for Biosystems Dynamics Research, Kobe 650-0047, Japan [15]The Institute of Medical Science, Asahi Life Foundation, Tokyo 100-0005, Japan

*Corresponding author. E-mail: ogawa@med.kobe-u.ac.jp (W. Ogawa).

Received March 7, 2024 • Revision received May 23, 2024 • Accepted June 11, 2024 • Available online 15 June 2024

https://doi.org/10.1016/j.molmet.2024.101968

We and others have identified two mouse and human PGC-1α variants (designated PGC-1αb and PGC-1αc, with the canonical form of PGC-1α designated PGC-1αa) that are produced by transcription from an alternative first exon (alternative exon 1, or AE1) [16—18] located upstream of the originally characterized exon 1 (exon 1a) (Figures 1A, S1A). The transcripts derived from the distal alternative promoter encode two different NH_2-terminal regions (consisting of 12 and 3 amino acids, respectively) that are shorter than that encoded by transcripts derived from the proximal promoter (16 amino acids). These variants differ from canonical PGC-1αa with regard to tissue distribution and mode of induction as a result of the difference in the corresponding promoters [16—19]. Whereas PGC-1αb and PGC-1αc derived from the alternative promoter manifest robust upregulation in skeletal muscle in response to exercise, PGC-1αa derived from the canonical promoter is induced by exercise to a much lesser extent [16,17,19]. Although the functions of the variant and canonical isoforms likely overlap in regulation of mitochondrial biogenesis, the different isoforms are also thought to have specific biological functions [20—23]. The precise differences in physiological functions between canonical PGC-1α and the variants have remained unclear, however. To provide insight into the role of the alternative variants of PGC-1α, we have now generated mice that specifically lack these variants by selectively disrupting AE1. We show here that such mice are prone to develop obesity, hyperinsulinemia, and cold intolerance as a result of a loss of the ability to adapt to external stimuli.

2. MATERIALS AND METHODS

2.1. Human subjects

Ten men with NGT and 10 men with T2D, the clinical characteristics of whom are presented in Table S1, were studied. The participants performed an acute bout of exercise on a cycle ergometer. The workload was set to 85% of their measured maximal heart rate, which was maintained for 30 min. Three hours after the exercise bout, muscle biopsy samples (40—100 mg) were obtained from the vastus lateralis with a Weil-Blakesley conchotome. The specimens were frozen immediately and stored in liquid nitrogen until analysis.

2.2. Mice

The PGC-1αAE1KO mice (Accession No. CDB0469K: https://large.riken.jp/distribution/mutant-list.html) in which AE1 of the PGC-1α gene was replaced with a floxed *neo* cassette (Figure S1, B and C) were generated using TT2 embryonic stem cells [24]. These mice were then bred with *Ella-Cre* transgenic mice, which express Cre recombinase in germ cells, in order to delete AE1 throughout the entire body of the resulting offspring. These latter mice were bred with C57BL/6J mice, and resulting offspring that did not harbor the *Cre* transgene were selected and then bred with C57BL/6J mice for six generations. The resulting heterozygotes for AE1 deletion were bred to obtain homozygotes for the deletion (PGC-1αAE1KO mice), with the offspring of such crosses being born at the expected Mendelian ratio. WT littermates were studied as control mice. Although the expression pattern of PGC-1α in male and female mice was similar, male mice were used for all subsequent data acquisition. For analysis under the static condition, mice at the indicated ages were killed in the randomly fed state between 9:00 and 11:00 a.m., unless indicated otherwise. For examination of the effects of acute exercise on gene expression, mice were subjected to forced exercise on a mouse treadmill at a speed of 15 m/min for 120 min.

2.3. GTT, food restriction, and assessment of skeletal muscle and fat mass

An intraperitoneal GTT was performed by administration of glucose (2 g/kg). Blood glucose levels were measured by glucose oxidase method (Sanwa Kagaku Kenkyusho). Serum levels of insulin were measured using insulin ELISA kit (Morinaga). For food restriction, PGC-1αAE1KO mice at 14—16 weeks of age were fed for 8 weeks with 80% of their previous daily food intake, whereas WT mice were fed ad libitum. The amounts of each type of fat tissue as well as skeletal muscle and lean body mass were determined by CT (LaTheta LCT-100M system, Aloka). CT scanning was performed at 0.6-mm intervals from the diaphragm to the bottom of the abdominal cavity.

2.4. Gene expression, immunoblot, and mtDNA analyses

Total RNA was extracted with the use of an RNeasy Mini Kit (Qiagen). The RNA was subjected to RT with the use of a high-capacity RT kit (Applied Biosystems), and the resulting cDNA was subjected to qPCR analysis with the use of SYBR Green PCR Master Mix and an ABI StepOne Plus Real-Time PCR system (Applied Biosystems). PGC-1α isoform mRNAs were subjected to quantification with the use of standard curves determined with plasmids containing the corresponding cDNAs so as to allow comparison of their amounts, and copy number was determined by quantitative real-time qPCR. The relative copy number of the transcripts was normalized to that of 36B4. The sequences of qPCR primer pairs for the PGC-1α variants are shown in Table S2. The expression of other genes was normalized by the amount of 36B4 mRNA as an internal control. Stable reference genes were identified using NormFinder software (https://www.moma.dk). The sequences of qPCR primer pairs are available on request. Immunoblot analysis was performed with antibodies to PGC-1α (ST1202, Calbiochem), to mitochondrial complex II (459200, Invitrogen), and to mitochondrial complex III (459140, Invitrogen), as well as with those to glyceraldehyde-3-phosphate dehydrogenase (GAPDH) as a loading control (M171-7, MBL). COS7 cells transfected with pcDNA3.1-based expression vectors encoding mouse PGC-1α isoforms and mouse PPARα were subjected to immunoprecipitation with antibodies to PGC-1α (ST1202, Calbiochem), and the resulting precipitates were subjected to immunoblot analysis with the same antibodies to PGC-1α and with those to PPARα (H-08, Santa Cruz Biotechnology). Mitochondrial DNA content was measured as the amount of cytochrome b copy number normalized to 36B4 gene copy number by qPCR.

2.5. Forced expression of PGC-1α in C2C12 myotubes by adenovirus infection

C2C12 myotubes that had been induced to differentiate by a standard protocol were infected for 48 h with recombinant adenoviruses encoding mouse PGC-1α isoforms or β-galactosidase (control). The cells were then subjected to RT-qPCR analysis, immunoblot analysis, or mitochondrial respiratory assays. Recombinant adenoviruses encoding PGC-1αa or β-galactosidase were described previously [25], and those encoding PGC-1αb, PGC-1αc, PGC-1α2, PGC-1α3, or PGC-1α4 were generated from the corresponding cDNAs (isolated by PCR from a mouse cDNA library) with the use of an Adenovirus Expression Vector Kit (Takara).

2.6. Assessment of mitochondrial function

The oxygen consumption rate of C2C12 myotubes or isolated mitochondria was measured with the use of an Oxygen Meter Model 781 and a Mitocell MT200 closed respiratory chamber (Strathkelvin Instruments). For C2C12 myotubes, the rate was measured in the

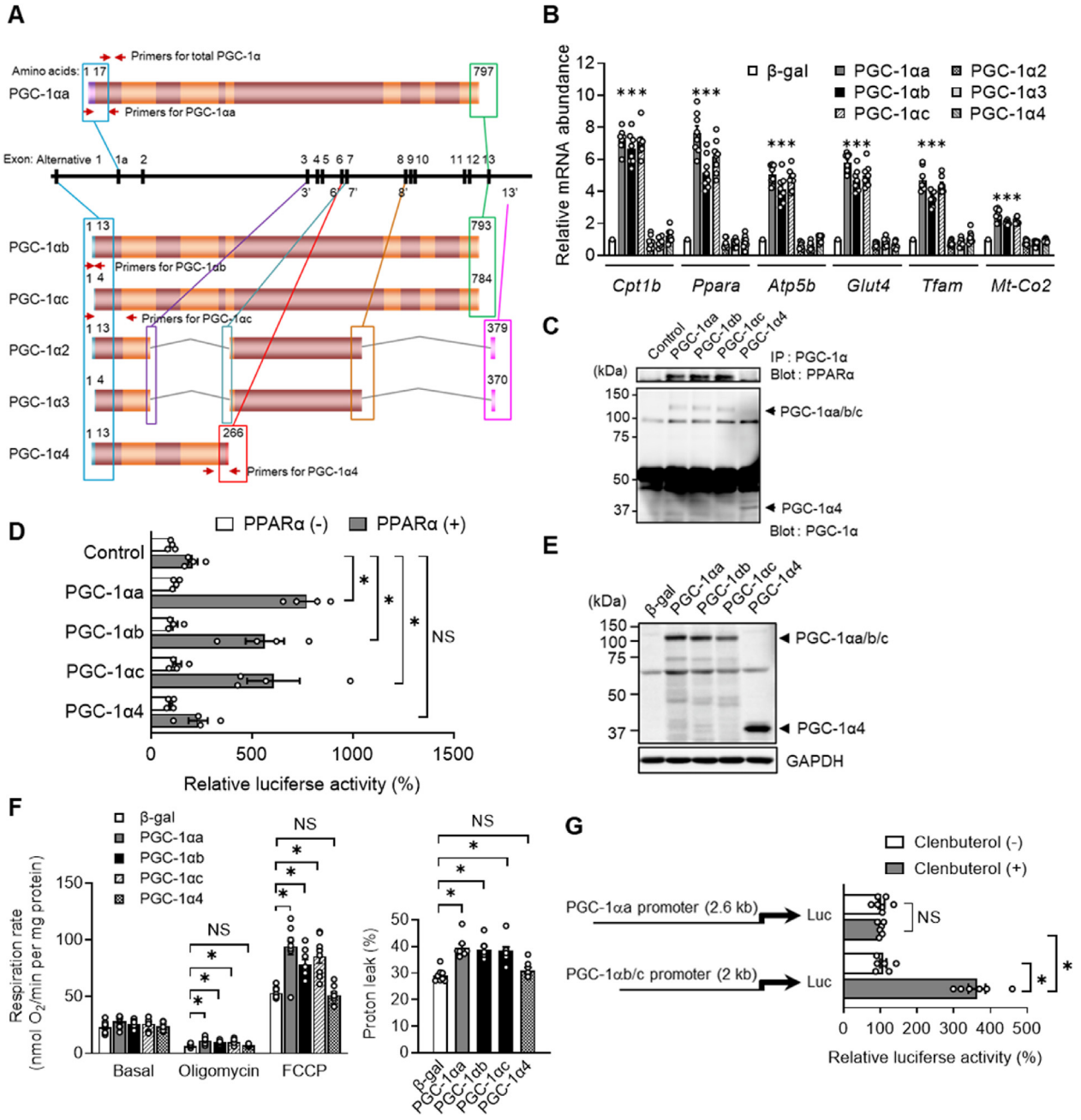

Figure 1: Molecular structures and functions of mouse PGC-1α isoforms. (A) Gene and predicted protein structures of PGC-1α isoforms. **(B)** C2C12 myotubes infected with adenoviruses encoding individual PGC-1α isoforms or β-galactosidase (β-gal, control) were subjected to RT-qPCR analysis of carnitine palmitoyltransferase 1b (*Cpt1b*), PPARα (*Ppara*), mitochondrial ATP synthase subunit β (*Atp5b*), glucose transporter 4 (*Glut4*), mitochondrial transcription factor A (*Tfam*), and cytochrome c oxidase subunit II (*Mt-Co2*) mRNAs ($n = 8$ independent experiments). The amount of each mRNA was normalized by that of 36B4 mRNA, and normalized values are expressed relative to the corresponding value for myotubes expressing β-gal. **(C)** COS7 cells transfected with expression vectors encoding each PGC-1α isoform (or with the corresponding empty vector, Control) and with an expression vector for mouse PPARα were subjected to immunoprecipitation (IP) with antibodies to PGC-1α, and the resulting precipitates were subjected to immunoblot analysis with antibodies to PPARα (upper panel) or to PGC-1α (lower panel). **(D)** Luciferase reporter assay with the reporter plasmid 3x-PPRE-luc for the transcriptional coactivator activity of PGC-1α isoforms expressed together with PPARα in C2C12 cells ($n = 4$ independent experiments). **(E, F)** C2C12 myotubes infected with adenoviruses encoding PGC-1α isoforms or β-gal (control) were subjected to immunoblot analysis of PGC-1α and GAPDH as a loading control (**E**) as well as assayed both for respiration rate under basal conditions and in the presence of oligomycin or carbonyl cyanide *p*-trifluoromethoxyphenylhydrazone (FCCP) and for mitochondrial proton leak (**F**) ($n = 8$ independent experiments). **(G)** Effects of clenbuterol on the promoter activity of PGC-1αa or PGC-1αb/c genes in C2C12 myoblasts. All quantitative data are means ± s.e.m. $^*P < 0.05$ versus the corresponding value for β-gal (B) or for the indicated comparisons (D, F) by one-way (B, F) or two-way (D, G) ANOVA with Bonferroni's post hoc test. NS, not significant.

absence or presence of the ATP synthase inhibitor oligomycin (6 μg/ml) or the uncoupling agent FCCP (5 μM). For mitochondria isolated from gastrocnemius muscle, state 2 respiration was measured with pyruvate and malate (each at 2.5 mM) as substrates, state 3 respiration was measured after the addition of ADP (0.25 mM) to the assay buffer, state 4 respiration was measured after the further addition of oligomycin (4 μg/ml), and uncoupled respiration was measured in the presence of FCCP (1 μM). The nonmitochondrial respiration rate determined by measurement of oxygen consumption in the presence of rotenone (1 μM) and myxothiazol (1 μM) was subtracted from each measured value. Proton leak (expressed as a percentage) was calculated by dividing the respiration rate in the presence of oligomycin by the basal respiration rate.

2.7. Luciferase reporter assay

Promoter regions for mouse PGC-1αa (nucleotides −1 to −2611, relative to the transcription start site) and PGC-1αb/c (−33 to −1969) were generated by PCR. The PCR productss were subcloned into pGL3 (Promega, Madison, WI). C2C12 myoblasts were transfected with the modified pGL3 vectors, as well as with an expression plasmid encoding β-galactosidase as an internal control. The cells were then incubated in the absence or presence of 1 μM clenbuterol (Sigma) for 4 h. C2C12 myoblasts were transfected with the reporter plasmid 3x-PPRE-luc (Addgene), pcDNA3.1 containing mouse PPARα cDNA, pcDNA3.1 containing mouse PGC-1α isoform cDNAs (or empty pcDNA3.1), and an expression plasmid encoding β-galactosidase as an internal control. Luciferase and β-galactosidase activities in cell lysates were measured 48 h after the onset of transfection with the use of a Luminescent β-Galactosidase Detection Kit II (Clontech). Luciferase activity was normalized by that of β-galactosidase.

2.8. Tissue pathology

Frozen muscle was sectioned in 8-μm thickness using a cryostat maintained. Serial sections were stained with hematoxylin and eosin and for reduced nicotinamide adenine dinucleotide-tetrazolium reductase (NADH-TR) to classify muscle fibers. The colorimetric intensity of NADH-TR activity in the muscle sections was quantified. WAT and BAT tissues were fixed in 10% neutral buffered formalin and routinely embedded in paraffin, sectioned, and stained with hematoxylin and eosin.

2.9. Determination of adipocyte size and number

Adipocyte size and number were measured after fixation of isolated adipocytes with osmium tetroxide, as described previously [26].

2.10. Food intake, energy expenditure, oxygen consumption, carbon dioxide production, and locomotor activity

The average daily food consumption of mice housed individually was determined over 7 days. Oxygen consumption, carbon dioxide production, and the respiratory quotient were determined with the use of an O_2/CO_2 respirometer system (Oxymax, Columbus Instruments). For determination of these parameters in the presence of a running wheel, mice were housed in the presence of the wheel for 2 days to allow acclimatization, and data obtained on the 3rd day were analyzed. Locomotor activity in the absence of a running wheel was determined with an infrared beam sensor, and that in the presence of a running wheel was estimated from the frequency of wheel rotation. For analysis of metabolic parameters during acute exercise, mice were allowed to acclimatize to the airtight treadmill chamber for 30 min and then made to run at a speed of 25 m/min for 30 min. Carbohydrate and lipids oxidation rates were calculated using the formulas: carbohydrate oxidation $= (4.55 \times VCO_2) - (3.21 \times VO_2)$, and lipid oxidation $= 1.67 \times (VO_2 - VCO_2)$ [27].

2.11. Measurement of motor performance

Motor performance of 3-month-old PGC-1αAE1KO and WT mice was assessed with an exercise endurance test with stepwise increases in treadmill rate. After acclimation (∼20 min), the mice were forced to run on a treadmill tilted at a 5° angle, starting at a speed of 10 m/min for 4 min. Each subsequent minute, the speed was increased by 1 m/min until the mice were exhausted. Exhaustion was defined as the inability of the animal to remain on the treadmill despite mechanical prodding. Running time and speed were measured, and the distance was calculated.

2.12. Effects of exercise training

Mice at 3 months of age were housed in the absence or presence of a running wheel for 6 weeks. They were then killed between 9:00 and 11:00 a.m., and isolated skeletal muscle was subjected to assays. For analysis of angiogenesis, capillaries in EDL were detected by immunostaining with antibodies to CD31 (550274, CiteAb) and the number of capillaries was counted in four random fields.

2.13. Measurement of intramuscular temperature

Mice were anesthetized, the dorsal subcutaneous was carefully dissected free, and the tip of the temperature probe was gently placed between the iliacus muscle and psoas major muscle and secured with two ligatures. The connector of the probe was tunneled subcutaneously to the back of the neck and connected to a BAT-12 Microprobe Thermometer (Physitemp, Clifton, NJ, USA). After the mice were allowed to recover for 1 day, intramuscular temperature was measured during exercise.

2.14. Statistics

Quantitative data were presented as means ± s.e.m. unless indicated otherwise and were analyzed by the two-tailed unpaired Student's *t* test, one-way or two-way analysis of variance (ANOVA) with Bonferroni's post hoc test, or Spearman's rank correlation test. All statistical analysis was performed with GraphPad Prism software version 9.0. A P value of <0.05 was considered statistically significant.

2.15. Study approval

All animal experiments were approved by the animal experimentation committee of Kobe University Graduate School of Medicine and the Institutional Animal Care and Use Committee of RIKEN Kobe Branch, and performed performed according to the guidelines of the each animal ethics committee. All human experiments were performed according to the Declaration of Helsinki and were approved by the medical ethics committee of the Karolinska Institutet, and all subjects provided written informed consent.

3. RESULTS

3.1. PGC-1αb and PGC-1αc have similar molecular functions to canonical PGC-1αa

Reverse transcription (RT) and quantitative polymerase chain reaction (qPCR) analysis revealed that PGC-1αa mRNA is relatively widely distributed among mouse tissues, whereas PGC-1αb and PGC-1αc mRNAs are largely restricted to brown adipose tissue (BAT), skeletal muscle, and heart (Figure S2A). Other variants of PGC-1α transcribed from AE1 have been identified and termed PGC-1α2, PGC-1α3, and PGC-1α4 (Figures 1A, S1A) [18]. PGC-1α2 and PGC-1α4 possess the

same NH_2-terminal sequence as does PGC-1αb, whereas PGC-1α3 possesses the same NH_2-terminal sequence as PGC-1αc. However, PGC-1α2 and PGC-1α3 lack exons 4 to 6 and 9 to 13, whereas PGC-1α4 lacks exons 7 to 13, with the result that each of these variants is much smaller than PGC-1αa, PGC-1αb, and PGC-1αc (Figures 1A, S1A).

To investigate the molecular functions of these PGC-1α isoforms, we examined the ability to induce gene expression in cultured cells. Forced expression of mouse PGC-1αb or PGC-1αc in mouse C2C12 myotubes increased the expression of genes related to mitochondrial function or to lipid or glucose metabolism to an extent similar to that triggered by PGC-1αa, whereas PGC-1α2, PGC-1α3, or PGC-1α4 did not activate the expression of these genes (Figure 1B). PGC-1αa, PGC-1αb, and PGC-1αc, but not PGC-1α4, associated with PPARα (Figure 1C) and increased the activity of this transcription factor (Figure 1D) in cultured cells. Moreover, overexpression of PGC-1αb or PGC-1αc in C2C12 myotubes increased respiratory capacity and proton leak of mitochondria to similar extents as did that of PGC-1αa (Figure 1E and F). β2-Adrenergic stimuli contribute to the expression of PGC-1αb and PGC-1αc in skeletal muscle [16]. The β2-adrenergic agonist clenbuterol stimulated the alternative promoter activities in cultured cells, whereas PGC-1α promoter activity was not affected (Figure 1G). These results collectively indicated that PGC-1αa, PGC-1αb, and PGC-1αc have similar molecular functions and that the functional differences between PGC-1αa and the alternative PGC-1αb/c are due to differences in the regulation of gene expression. The short isoforms PGC-1α2, PGC-1α3, and PGC-1α4, however, appear not to possess metabolic functions common to the other three isoforms.

3.2. PGC-1αb and PGC-1αc account for exercise-induced upregulation of PGC-1α in mouse and human skeletal muscle

Treadmill exercise resulted in marked increases in the abundance of PGC-1αb and PGC-1αc mRNAs as well as in the total abundance of PGC-1α mRNA, whereas the amount of PGC-1αa mRNA was not significantly affected, in mouse skeletal muscle (Figure 2A). The abundance of PGC-1α4 mRNA in mouse skeletal muscle was too low for accurate quantitative analysis. The expression pattern of PGC-1α in male and female mice was similar (Figures 2A and S2B). Exercise load with an ergometer in human individuals with normal glucose tolerance (NGT) or type 2 diabetes mellitus (T2D) resulted in significant increases in the abundance of PGC-1ab and PGC-1αc mRNAs as well as total PGC-1α mRNA, but not in that of PGC-1αa mRNA (Figure 2B). Individuals with T2D showed a reduced level of PGC-1α gene expression in skeletal muscle relative to those with NGT. The amount of PGC-1α4 mRNA in skeletal muscle of individuals with NGT or T2D was also upregulated in response to exercise, but this increase was too small to substantially affect the total abundance of PGC-1α mRNA (Figure 2B). The total abundance of PGC-1α mRNA as well as the amounts of PGC-1αb and PGC-1αc mRNAs were positively correlated with the maximal rate of oxygen consumption ($\dot{V}O_2$ max) during ergometer exercise (Figure 2C) and tended to be negatively correlated with percentage body fat (Figure S3), whereas the amounts of PGC-1αa and PGC-1α4 mRNAs were not. Collectively, these results suggested that PGC-1αb and PGC-1αc account for the exercise-induced upregulation of PGC-1α expression in skeletal muscle and consequently contribute to oxygen consumption during exercise in both mice and humans.

3.3. Mice lacking AE1 of the PGC-1α gene develop obesity and hyperinsulinemia

To shed light on the physiological functions of PGC-1α isoforms transcribed from AE1, we generated mice that lack this exon (PGC-1αAE1KO mice) (Figure S1, B and C). Transcripts encoding PGC-1αb, PGC-1αc, or PGC-1α4 were not detected in these animals (Figure S4A). The amounts of mRNAs for PGC-1αa and for PGC-1β, a structural and functional homolog of PGC-1α encoded by a different gene, were unaltered in various tissues of PGC-1αAE1KO mice (Figure S4, B and C).

The body mass of PGC-1αAE1KO mice increased to a greater extent with age compared with that of wild-type (WT) mice (Figure 3A). The mass of isolated epididymal white adipose tissue (eWAT) (Figure 3B) as well as total abdominal adipose tissue mass assessed by computed tomography (CT) (Figure 3C) were also greater for PGC-1αAE1KO mice than for WT mice. The mass of isolated gastrocnemius muscle and lean body mass were similar between WT and PGC-1αAE1KO mice (Figure 3B and D). The size of eWAT adipocytes (Figure 3E–G) was increased and that of subcutaneous adipocytes tended to be increased (Figure 3F and G) in the mutant mice compared with WT mice. Food intake was similar in mice of both genotypes (Figure 3H), as were blood glucose (Figure 3I) and plasma insulin (Figure 3J) concentrations in the randomly fed state. A glucose tolerance test (GTT) revealed no significant difference in blood glucose concentrations between PGC-1αAE1KO and WT mice (Figure 3K), whereas plasma insulin levels were higher in the mutant animals (Figure 3L), indicative of insulin resistance. To examine whether hyperinsulinemia of PGC-1αAE1KO mice is attributable to obesity, we subjected the animals to food restriction. PGC-1αAE1KO mice were thus fed for 8 weeks with ∼80% of the amount of chow they had previously consumed, whereas WT mice were fed ad libitum. After the period of food restriction, body mass as well as blood glucose and plasma insulin levels during the GTT for the PGC-1αAE1KO mice were similar to those for the WT mice (Figure S5, A–C), suggesting that obesity may contribute the cause of hyperinsulinemia in the mutant animals.

Under the static condition, the total abundance of PGC-1α mRNA in skeletal muscle was only slightly (5–10%) smaller for PGC-1αAE1KO mice than for WT mice (Figure 3M), likely because PGC-1αa is the predominant PGC-1α isoform in skeletal muscle under this condition. The amount of mitochondria, as assessed by measurement of mitochondrial DNA (mtDNA), was also reduced in extensor digitorum longus (EDL) and gastrocnemius muscles of PGC-1αAE1KO mice to an extent similar to that apparent for total PGC-1α mRNA (Figure 3N). Furthermore, respiration rate in state 4 and proton leak were reduced for mitochondria isolated from skeletal muscle of PGC-1αAE1KO mice (Figure 3O). However, the morphology of mitochondria and expression of mitochondrial proteins in skeletal muscle appeared to be unaltered in PGC-1αAE1KO mice (Figure S6, A and B). The fiber-type composition of skeletal muscle as assessed either by RT-qPCR analysis of myosin heavy chain (MHC) gene expression (Figure S6C) or by reduced nicotinamide adenine dinucleotide (NADH)–dependent tetrazolium reductase staining (Figure S6, D and E) also did not differ significantly between the two mouse genotypes.

3.4. Upregulation of energy expenditure in the dark phase is attenuated in PGC-1αAE1KO mice

The extent and circadian pattern of locomotor activity were unaltered in PGC-1αAE1KO mice, with the amount of locomotor activity being increased during the dark phase in mice of both genotypes compared with that during the light phase (Figure 4A and F). The abundance of PGC-1αb and PGC-1αc mRNAs, but not that of PGC-1αa and PGC-1α4 mRNAs, in skeletal muscle of WT mice was higher in the dark phase of the circadian cycle than in the light phase (Figure 4B). Oxygen consumption and heat production in the dark phase, but not those in the light phase, were both attenuated in PGC-1αAE1KO mice compared

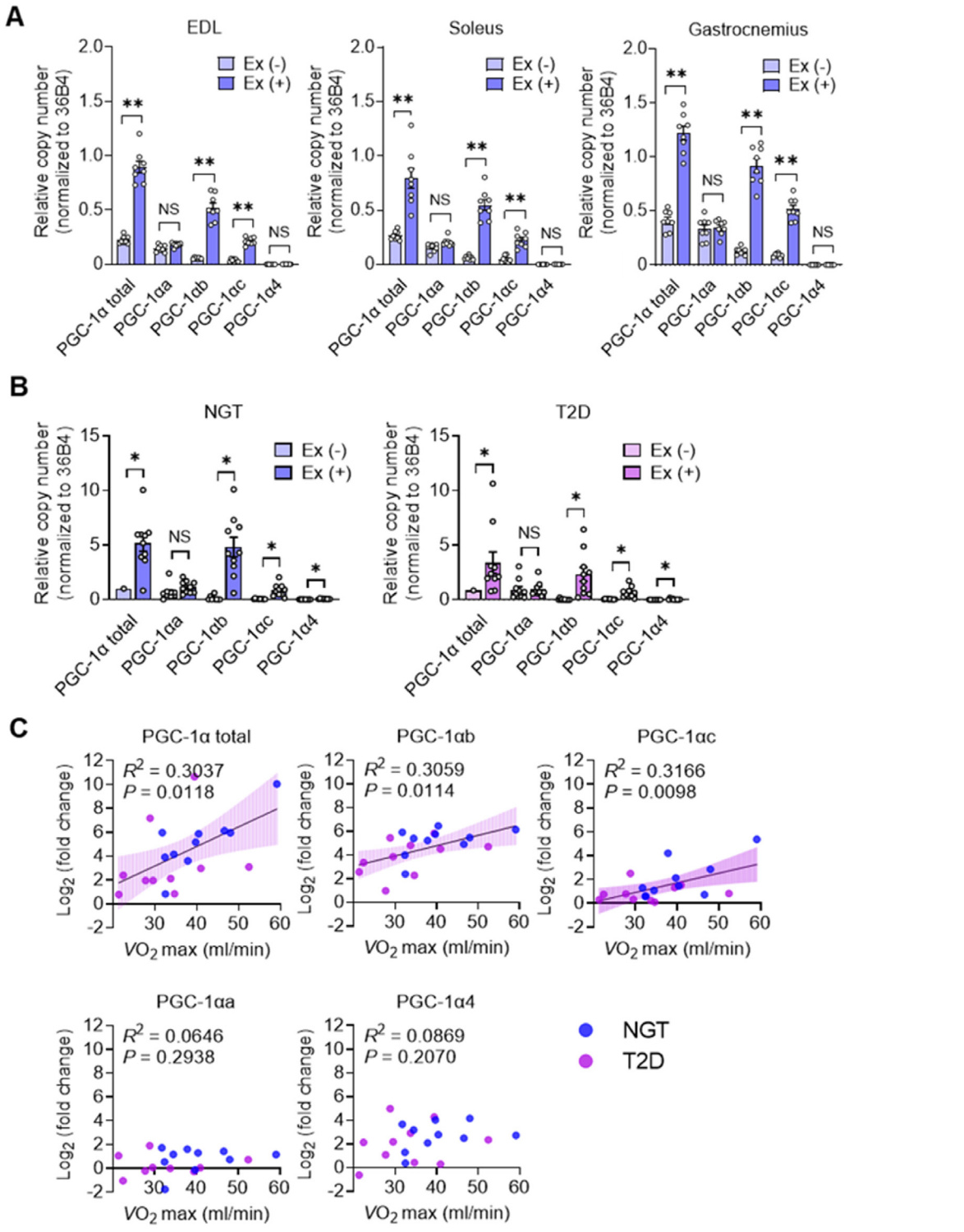

Figure 2: Effects of exercise on the abundance of PGC-1α isoform mRNAs in mice and humans. (A) RT-qPCR analysis of PGC-1α isoform mRNAs in skeletal muscle of male C57BL/6J mice both under the static condition (Ex (−)) and after exercise on a treadmill at 15 m/min for 120 min (Ex (+)) ($n = 8$ mice per group). EDL, extensor digitorum longus. **(B)** RT-qPCR analysis of PGC-1α isoform mRNAs in vastus lateralis skeletal muscle of human individuals with NGT ($n = 10$) or T2D ($n = 10$) both under the static condition (Ex (−)) and after ergometer exercise for 30 min (Ex (+)). PGC-1α isoform mRNAs were subjected to quantification with the use of standard curves determined with plasmids containing the corresponding cDNAs so as to allow comparison of their amounts, and copy number was determined by RT-qPCR. The relative copy number of the transcripts was normalized to that of 36B4. Data in (A) and (B) are means ± s.e.m. $^*P < 0.05$, $^{**}P < 0.01$, and NS by one-way ANOVA with Bonferroni's post hoc test. **(C)** Correlation of log$_2$[fold change] for the exercise-induced increase in the abundance of PGC-1α isoform mRNAs in human skeletal muscle and VO_2 max (NGT, $n = 10$; T2D, $n = 10$). Spearman correlation R^2 values and P values are indicated.

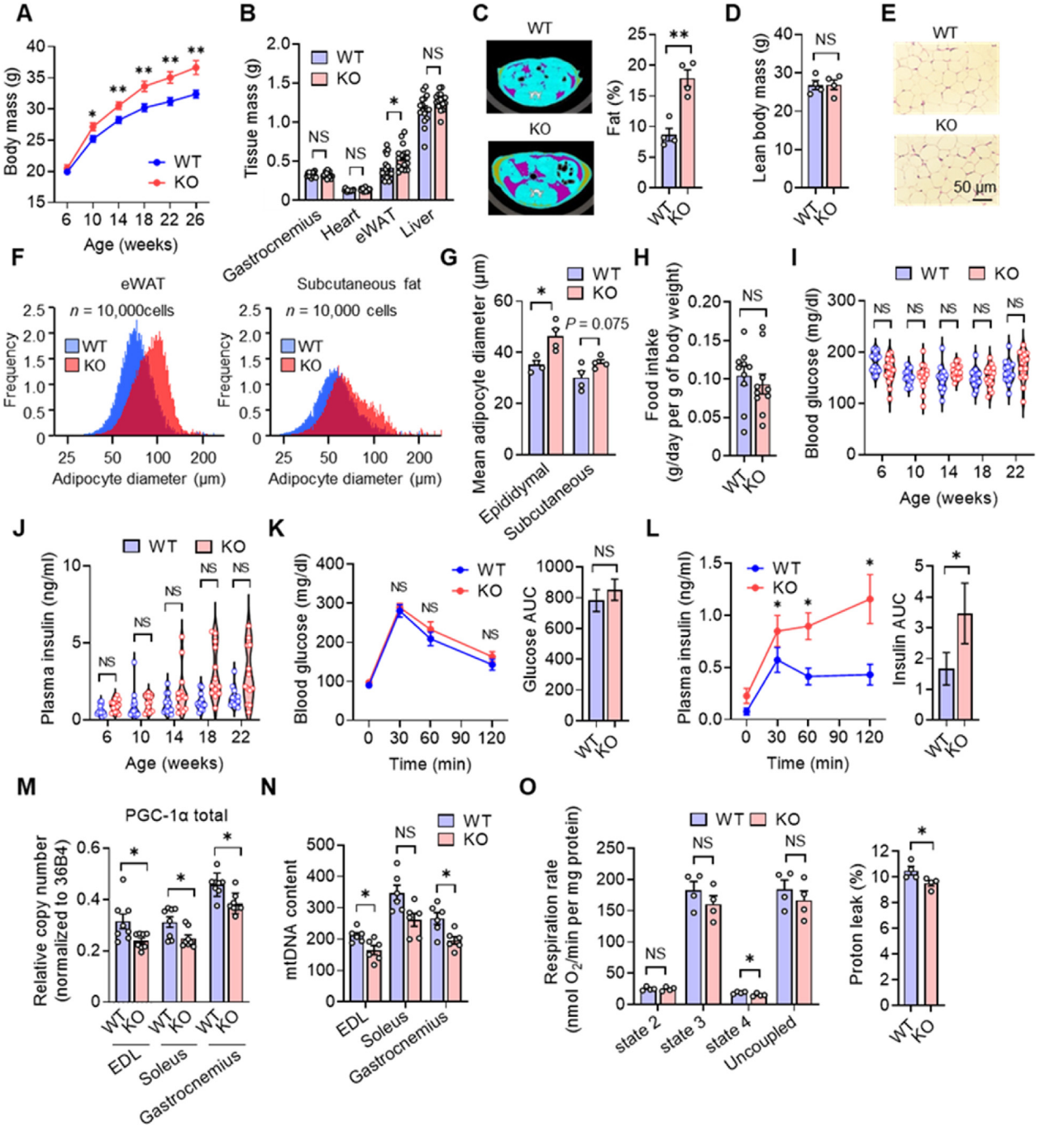

Figure 3: Obesity and insulin resistance in PGC-1αAE1KO mice. (A—D) Body mass at the indicated ages ($n = 16$) (A), tissue mass at 4 months of age ($n = 16$) (B), as well as abdominal images and adipose tissue mass ($n = 4$) (C) and lean body mass ($n = 4$) (D) obtained by CT at 4 months of age for WT and KO mice. **(E—G)** Hematoxylin—eosin staining of eWAT (E) as well as adipocyte diameter in epididymal or subcutaneous fat as determined either with a Coulter counter (F) or by histological analysis (G) for WT and KO mice at 3 months of age ($n = 4$). **(H)** Food intake for 4-month-old WT and KO mice ($n = 10$). **(I, J)** Violin plots for blood glucose (I) and plasma insulin (J) concentrations in the randomly fed state and at the indicated ages ($n = 16$). Plot center lines denote the median. **(K, L)** Blood glucose (K) and plasma insulin (L) levels during an *intra*peritoneal GTT (left panels) as well as the corresponding area under the curve (AUC) values (right panels) for WT and KO mice at 7 months of age ($n = 11$). **(M, N)** RT-qPCR analysis of total PGC-1α mRNA ($n = 8$) (M) and qPCR analysis of mtDNA content ($n = 6$) (N) for the indicated skeletal muscles of WT and KO mice at 4 months of age. **(O)** Function of mitochondria isolated from gastrocnemius muscle of WT and KO mice at 4 months of age ($n = 4$). Quantitative data are means ± s.e.m. for the indicated numbers (n) of mice in (A—D, G, H—O). $^{*}P < 0.05$, $^{**}P < 0.01$, and NS versus the corresponding WT value or for the indicated comparisons by the two-tailed unpaired Student's *t* test (B—D, H—J; K,L (right panels)) or by one-way (A; K, L (left panels); M-O) or two-way (G) ANOVA with Bonferroni's post hoc test.

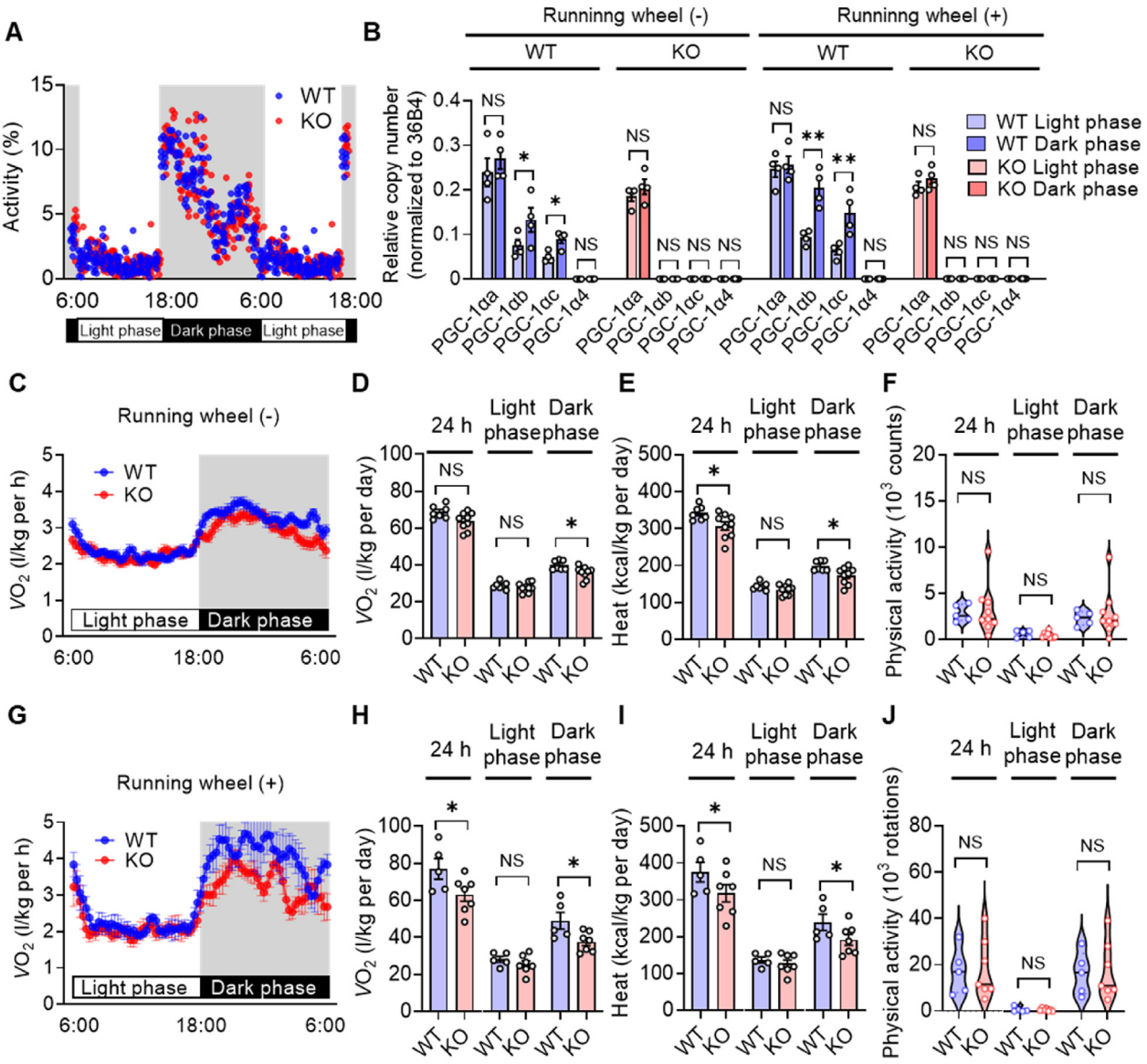

Figure 4: Oxygen consumption, heat production, and locomotor activity during the light and dark phases for PGC-1αAE1KO mice. (A) The circadian pattern of locomotor activity for WT and KO mice at 3 months of age was analyzed with an infrared sensor for 10 days ($n = 10$). Locomotor activity is expressed as a percentage of the daily total: 100% × (activity counts for each hour/total activity counts for 24 h). Each point corresponds to an individual mouse. **(B)** RT-qPCR analysis of PGC-1α isoform mRNAs in skeletal muscle of WT and KO mice during the light and dark phases in the absence or presence of a running wheel ($n = 4$). **(C—E, G—I)** Circadian pattern of oxygen consumption ($\dot{V}O_2$) (C, G) as well as the levels of oxygen consumption (D, H) and heat production (E, I) during the light and dark phases in the absence (WT, $n = 7$; KO, $n = 9$) (C—E) or presence (WT, $n = 5$; KO, $n = 7$) (G—I) of a running wheel for 4-month-old WT and KO mice. **(F, J)** Locomotor activity for 4-month-old WT and KO mice during the light and dark phases was analyzed for 4 days in the absence (WT, $n = 7$; KO, $n = 9$) (F) or presence (WT, $n = 5$; KO, $n = 7$) (J) of a running wheel. The center lines of the violin plots indicate the median. Data are means ± s.e.m. in (B—E, G—I), and n values indicate the numbers of mice. $^*P < 0.05$, $^{**}P < 0.01$, and NS by the two-tailed unpaired Student's t test (D—F, H—J) or two-way ANOVA with Bonferroni's post hoc test (B).

with WT mice (Figure 4C—E). Housing of mice in the presence of a running wheel increases voluntary activity and energy expenditure. In the presence of a running wheel, the upregulation of PGC-1αb and PGC-1αc mRNAs in skeletal muscle of WT mice apparent in the dark phase was enhanced (Figure 4B). The differences in oxygen consumption and heat production between WT and PGC-1αAE1KO mice during the dark phase were also more prominent in the presence of a running wheel (Figure 4, G—I). The frequency of wheel rotation was similar for the two genotypes (Figure 4J). These results suggested that the exercise-induced increase in energy expenditure is attenuated in PGC-1αAE1KO mice, likely contributing to their obesity-prone phenotype. PGC-1αAE1KO mice housed with or without a running wheel showed a respiratory quotient similar to that of WT mice (Figure S7, A and B).

3.5. The exercise-induced increase in energy expenditure is attenuated in PGC-1αAE1KO mice

To confirm that the exercise-induced increase in energy expenditure is indeed attenuated in PGC-1αAE1KO mice, we investigated the effects of forced treadmill exercise. We first examined the motor performance of PGC-1αAE1KO mice. The reduced capacity of the mutant mice for exercise was confirmed in a treadmill test with a load-increasing

protocol (Figure 5A–C). Whereas both WT and PGC-1αAE1KO mice were able to complete treadmill exercise at a rate of 15 m/min for 120 min, the mutant animals were less able to withstand greater exercise loads. We next measured oxygen consumption by PGC-1αAE1KO mice during treadmill exercise at a rate of 25 m/min, an exercise load that both WT and mutant mice were able to withstand. PGC-1αAE1KO mice manifested reduced oxygen consumption during the exercise load compared with WT animals (Figure 5D and E). PGC-1αAE1KO mice subjected to treadmill exercise tended to have a slightly increased respiratory quotient (Figure S7C), consistent with a shift toward reduced use of fat relative to carbohydrate as a fuel (Figure 5F and G). Consistent with the notion that PGC-1αAE1KO mice consume less energy during exercise, the reductions in body mass and eWAT mass induced by exercise load were smaller in the mutant mice than in WT animals (Figure 5H and I). Moreover, the increase in intramuscular temperature during treadmill exercise was attenuated in PGC-1αAE1KO mice (Figure 5J), suggestive of impaired heat production by skeletal muscle.

The amount of total PGC-1α mRNA in skeletal muscle after exercise was markedly smaller for PGC-1αAE1KO mice than for WT mice, with the WT animals showing large exercise-induced increases in the abundance of PGC-1αb and PGC-1αc mRNAs (Figure 5K). Immunoblot analysis revealed that exercise increased the intensity of a band at ∼100 kDa (corresponding to the molecular size of PGC-1αa, PGC-1αb, and PGC-1αc) in skeletal muscle of WT mice, whereas this effect was greatly attenuated in PGC-1αAE1KO mice (Figure 5L). Expression of the gene for uncoupling protein 3 (*Ucp3*), a protein related to proton leak, was also increased in skeletal muscle of WT mice in response to exercise, whereas this increase was attenuated in the mutant mice (Figure 5M). Furthermore, PGC-1αAE1KO mice showed impairment of exercise-induced expression in skeletal muscle of genes related to lipid metabolism—including those for PPARα (*Ppara*), PPARδ (*Ppard*), estrogen-related receptor α (*Erra*), acyl-CoA thioesterase 1 (*Acot1*), and medium-chain acyl-CoA dehydrogenase (*Mcad*) (Figure 5M)—supporting the notion that PGC-1α variants transcribed from AE1 contribute to the adaptive response of energy metabolism in skeletal muscle to exercise.

Exercise is also thought to induce beneficial changes in adipose tissue. The amounts of total PGC-1α and PGC-1αa mRNAs (Figure S8, A and B) as well as the expression of various genes related to lipid and energy metabolism (Figure S8, C and D) in eWAT and subcutaneous fat of WT mice were increased in response to exercise. These exercise-induced changes in gene expression were not attenuated in PGC-1αAE1KO mice, consistent with the observation that the abundance of PGC-1αb, PGC-1αc, and PGC-1α4 mRNAs is small in these tissues. Exercise also increases the expression of thermogenesis-related genes in white adipocytes and stimulates browning of WAT [28], with these effects being mediated in part by PGC-1α [29]. We found that the exercise-induced expression of genes related to thermogenesis or the browning of WAT—including those for *Ucp1*, *Cidea*, and *Prdm16*—was unaffected in PGC-1αAE1KO mice (Figure S8, C and D). We also investigated the effect of acute exercise on PGC-1α gene expression in BAT. The amounts of PGC-1αb and PGC-1αc mRNAs were increased, whereas those of PGC-1αa and total PGC-1α mRNAs were decreased, by exercise in BAT of WT mice (Figure S8E). The abundance of total PGC-1α and PGC-1αa mRNAs in BAT of PGC-1αAE1KO mice was also reduced after exercise. These results suggested that adipose tissue is not responsible for the impaired energy expenditure of PGC-1αAE1KO mice during exercise.

3.6. BAT function during cold exposure is impaired in PGC-1αAE1KO mice

The mass and histology of, as well as total PGC-1α mRNA abundance in, BAT were unaltered in PGC-1αAE1KO mice under basal conditions (Figure 6A–C). Cold exposure increased the amounts of total PGC-1α as well as PGC-1αb and PGC-1αc mRNAs, but not those of PGC-1αa and PGC-1α4 mRNAs, in BAT of WT mice, whereas such induction of total PGC-1α mRNA was impaired in PGC-1αAE1KO mice (Figure 6C). Whereas the amount of *Ucp1* mRNA in BAT was similar for WT and PGC-1αAE1KO mice under basal conditions, it was significantly lower in PGC-1αAE1KO mice than in WT mice after cold exposure (Figure 6D). Moreover, PGC-1αAE1KO mice showed an exaggerated drop in body temperature during cold exposure (Figure 6E). These results suggested that PGC-1αb and PGC-1αc play an important role in maintenance of body temperature during cold adaptation.

PGC-1α is induced in response to cold exposures also in eWAT [30]. The amounts of total PGC-1α and PGC-1αa mRNAs were thus increased in eWAT of WT mice after cold exposure (Figure 6F). The amounts of PGC-1αb, PGC-1αc, and PGC-1α4 mRNAs in this tissue were small both before and after exposure to a cold environment. The increases in the abundance of total PGC-1α and PGC1-αa mRNAs induced by cold exposure were unaltered in PGC-1αAE1KO mice, as was the expression of genes related to energy metabolism or browning of WAT, including *Ucp1*, *Ucp2*, *Ucp3*, *Prdm16*, and *Cidea* (Figure 6G). These findings suggested that the cold intolerance of PGC-1αAE1KO mice is attributable to insufficient function of BAT, not to that of eWAT or beige adipocytes.

3.7. Effect of exercise training on remodeling of skeletal muscle in PGC-1αAE1KO mice

PGC-1α is thought to contribute to remodeling of skeletal muscle in response to chronic exercise training [31]. We therefore investigated the effects of exercise training in PGC-1αAE1KO mice. Housing of WT mice in the presence of a running wheel for 6 weeks increased the percentage of slow-twitch fibers (Figure 7A), the amount of mitochondria (Figure 7B), and vascular density (Figure 7C and D) in skeletal muscle. PGC-1αAE1KO mice also manifested similar changes in response to such exercise training (Figure 7A–D). Exercise training upregulated PGC-1αa mRNA but not PGC-1αb and PGC-1αc mRNAs in skeletal muscle of WT mice, with the total amount of PGC-1α mRNA after training being similar in WT and PGC-1αAE1KO mice (Figure 7E). These results suggested that upregulation of PGC-1αa compensated for the lack of the novel variants during skeletal muscle remodeling—in terms of the increases in the percentage of slow-twitch fibers, the amount of mitochondria, and vascular density—induced by exercise training.

4. DISCUSSION

We have here shown that mice lacking AE1 of the PGC-1α gene (PGC-1αAE1KO mice) are prone to the development of obesity and hyperinsulinemia. Energy expenditure by these mice was attenuated both during forced exercise as well as in the dark phase, when mice are active. Moreover, the exercise-induced increase in the temperature of skeletal muscle was smaller in the mutant mice than in WT mice. These results suggest that the exercise-induced upregulation of the PGC-1αb and PGC-1αc variant isoforms and consequent increase in energy expenditure are essential for the regulation of whole-body energy metabolism. This notion was also supported by our finding

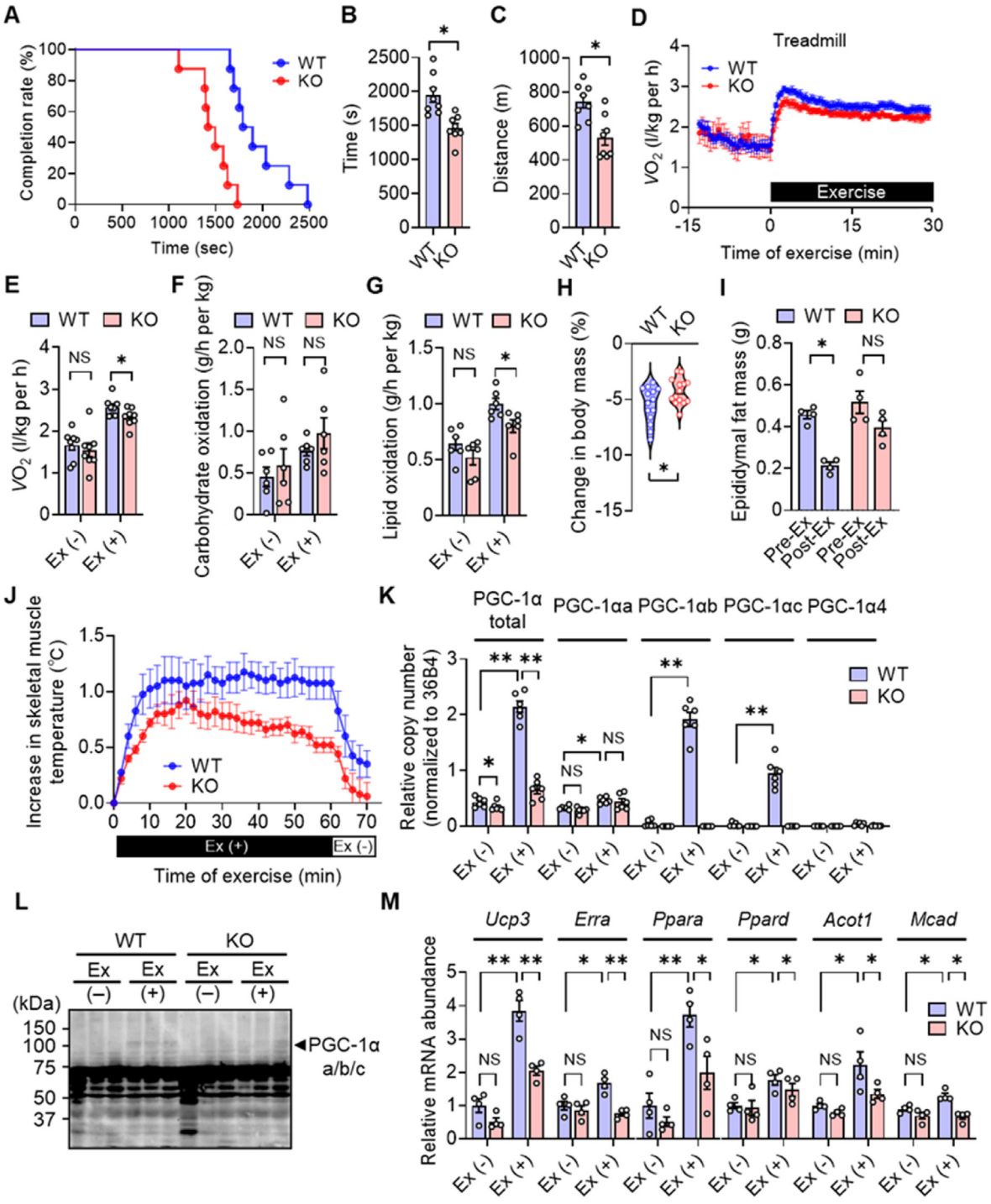

Figure 5: Impaired motor performance as well as attenuated exercise-induced energy expenditure and gene expression in PGC-1αAE1KO mice. (A–C) Motor performance of 3-month-old WT and KO mice ($n = 8$) was assessed by an exercise endurance test with stepwise increases in treadmill rate (A). Exhaustion was defined as the inability of the animal to remain on the treadmill despite mechanical prodding. The average time (B) and distance (C) of running until exhaustion were determined. **(D–G)** Time course of oxygen consumption ($n = 8$) (D), total oxygen consumption ($n = 8$) (E), carbohydrate oxidation rate ($n = 6$) (F), and lipid oxidation rate ($n = 6$) (G) during the first 30 min of forced treadmill exercise (Ex) at 25 m/min for 4-month-old WT and KO mice. **(H, I)** Percentage change in body mass ($n = 14$) after (H), and epididymal fat mass ($n = 4$) before and after (I), forced treadmill exercise for 120 min at 15 m/min for 4-month-old WT and KO mice. **(J)** Intramuscular temperature of 4-month-old WT and KO mice during forced treadmill exercise at 15 m/min ($n = 5$). **(K, L)** RT-qPCR analysis of PGC-1α isoform mRNAs in gastrocnemius muscle ($n = 6$) (K) and immunoblot analysis of PGC-1α in EDL ($n = 3$) (L) for 4-month-old WT and KO mice under the static condition (Ex (−)) or after forced treadmill exercise at 15 m/min for 120 min (Ex (+)). **(M)** RT-qPCR analysis of mRNAs for the indicated genes in gastrocnemius muscle of 4-month-old WT and KO mice under the static condition or after forced treadmill exercise at 15 m/min for 120 min ($n = 4$). The amount of each mRNA was normalized by that of 36B4 mRNA, and normalized values are expressed relative to the corresponding value for WT Ex (−). All quantitative data are means ± s.e.m. for the indicated numbers (n) or mice with the exception of those in (A) and (H), with the median being indicated in (H). $^*P < 0.05$, $^{**}P < 0.01$, and NS by the two-tailed unpaired Student's t test (B, C, H) or two-way ANOVA with Bonferroni's post hoc test (E–G, I, K, M).

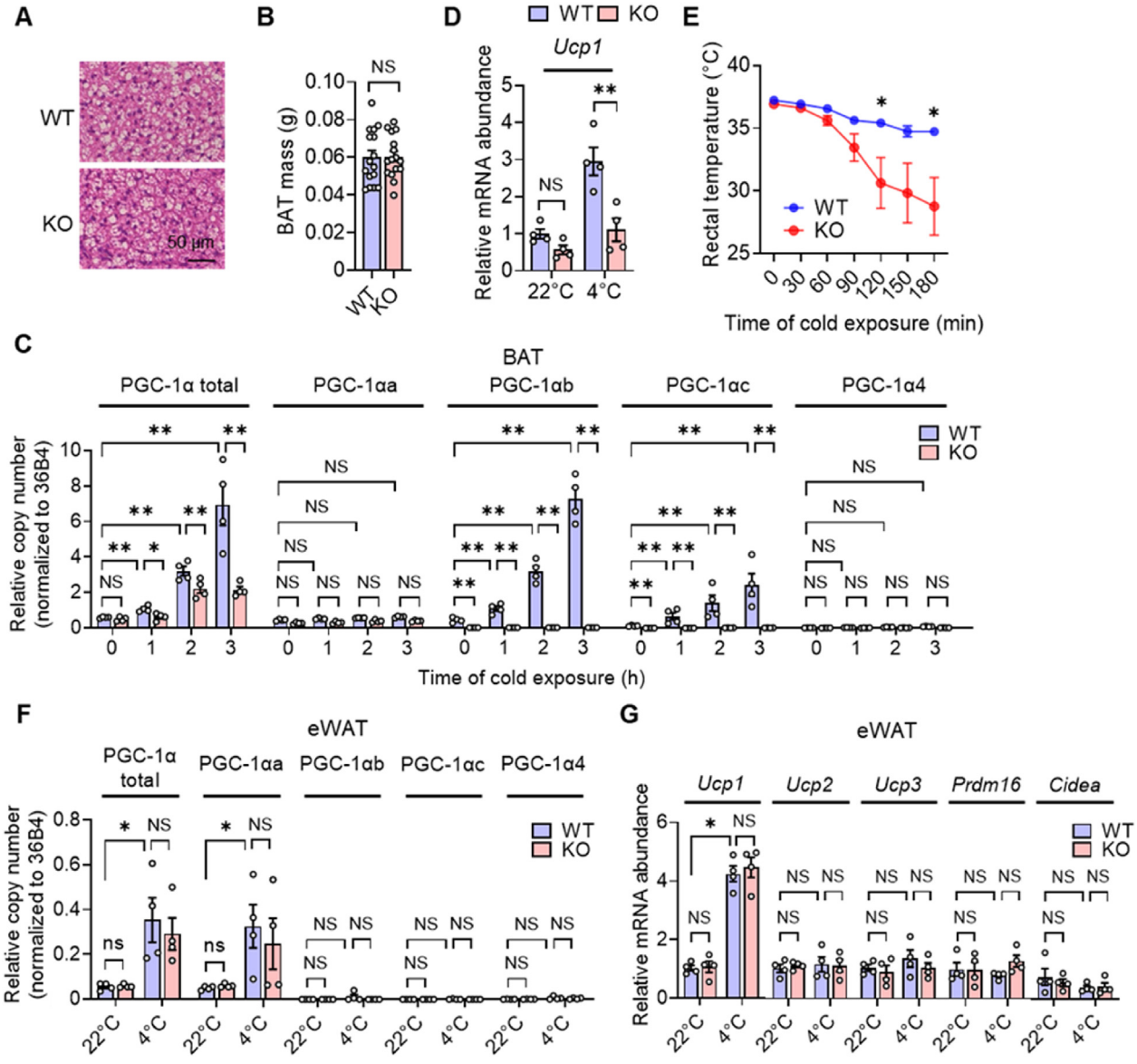

Figure 6: Characterization of BAT and change in body temperature in response to cold exposure in PGC-1αAE1KO mice. (A, B) Hematoxylin—eosin staining (A) and tissue mass ($n = 16$) (B) for interscapular BAT of WT and KO mice at 8 weeks of age. **(C, D)** RT-qPCR analysis of PGC-1α isoform mRNAs ($n = 4$) (C) and of UCP1 mRNA ($n = 4$) (D) in BAT of 6-week-old WT and KO mice maintained either at 22 °C or for the indicated times (C) or 3 h (D) at 4 °C. The amount of UCP1 mRNA was normalized by that of 36B4 mRNA, and normalized values are expressed relative to the value for WT at 22 °C. **(E)** Rectal temperature of 6-week-old WT and KO mice during exposure to 4 °C for the indicated times ($n = 6$). **(F, G)** RT-qPCR analysis of PGC-1α isoform mRNAs (F) and of expression of the indicated genes (G) in eWAT of 4-month-old WT and KO mice maintained at 22 °C or for 3 h at 4 °C ($n = 4$). Gene expression in (G) was normalized by the amount of 36B4 mRNA, and normalized values are expressed relative to the value for WT at 22 °C. All quantitative data are means ± s.e.m. for the indicated numbers (n) or mice. $^*P < 0.05$, $^{**}P < 0.01$, and NS versus the corresponding value for KO mice (E) or for the indicated comparisons (B—D, F, G) by the two-tailed unpaired Student's t test (B) or two-way ANOVA with Bonferroni's post hoc test (C—G).

that exercise-induced energy expenditure and the abundance of PGC-1αb and PGC-1αc mRNAs in skeletal muscle are significantly correlated in humans. When we searched the NCBI database, we found that PGC-1α is conserved in organisms other than mammals, including nematodes and fruit flies. However, PGC-1α variants with different N termini have not been identified in non-mammalian species. This may reflect evolutionary adaptations to external stimuli in different species. Forced expression of PGC-1αb or PGC-1αc in C2C12 myotubes increased mitochondrial proton leak, with such an effect likely contributing to energy consumption and heat production in skeletal muscle. The exercise-induced expression of the gene for UCP3, which regulates respiratory uncoupling and proton leak [32], was attenuated in skeletal muscle of PGC-1αAE1KO mice. Transgenic mice that overexpress UCP3 in skeletal muscle are protected from obesity [33,34], whereas mice lacking this protein manifest increased fat storage after long-term feeding with a high-fat diet compared with WT mice [35]. The impaired exercise-induced induction of *Ucp3* may therefore contribute, at least in part, to the development of obesity in PGC-1αAE1KO mice. However, mice lacking UCP3 do not manifest frank obesity during normal chow feeding [36,37], which may implicate additional molecules or pathways in the obesity-prone phenotype of PGC-1αAE1KO mice.

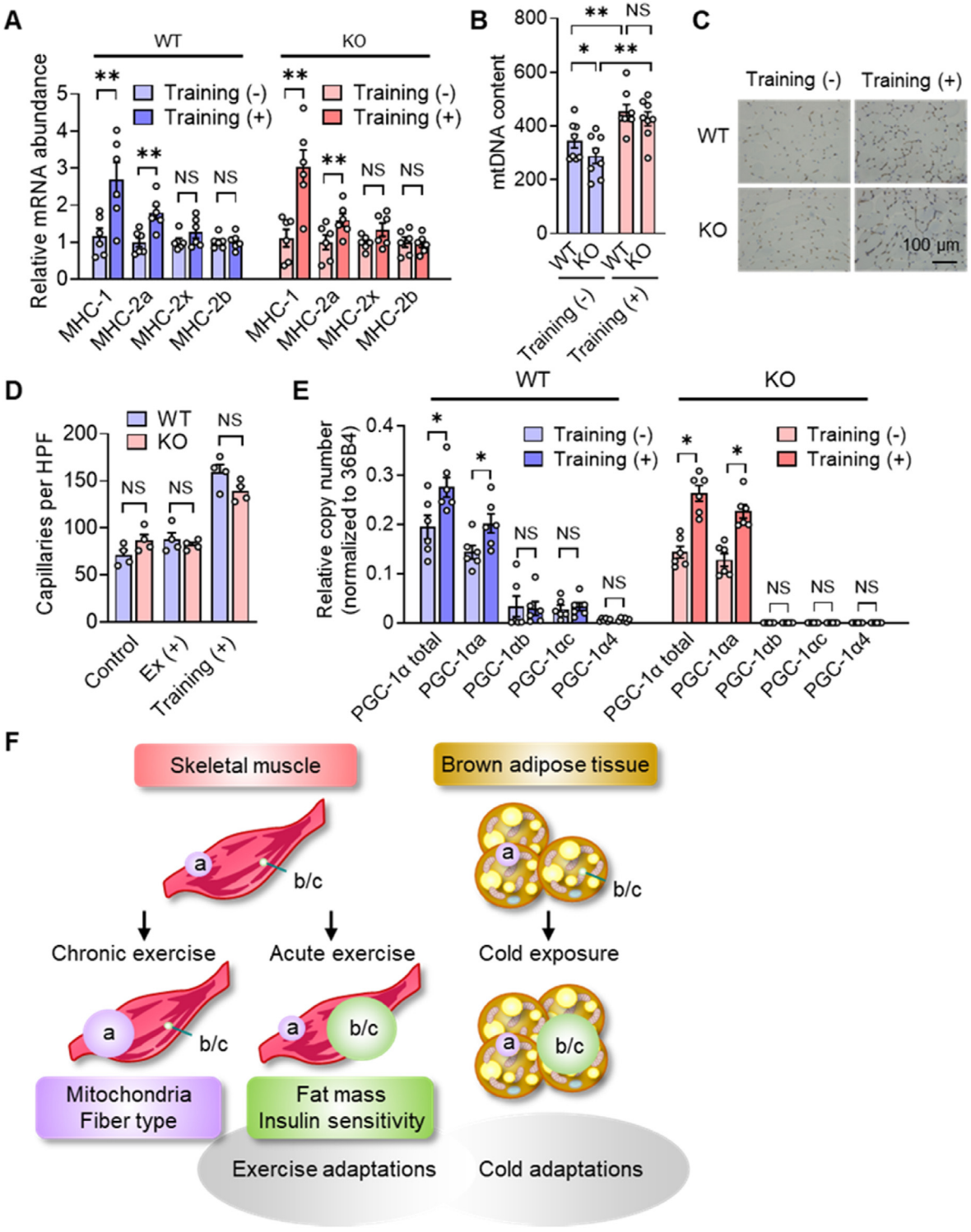

Figure 7: Effects of exercise training on skeletal muscle remodeling in PGC-1αAE1KO mice. (A, B) RT-qPCR analysis of MHC mRNAs ($n = 6$) (A) and qPCR analysis of mtDNA ($n = 8$) (B) in gastrocnemius of WT and KO mice maintained with or without exercise training for 6 weeks beginning at 3 months of age. The amount of each MHC mRNA was normalized by that of 36B4 mRNA, and normalized values are expressed relative to the corresponding value for training (−). **(C, D)** Vascular density in EDL as determined by immunohistochemical staining with antibodies to CD31 (C) and represented by the average number of CD31-positive capillaries per high-power field (HPF) among four such HPFs (D) for WT and KO mice ($n = 4$) maintained with or without exercise training for 6 weeks beginning at 3 months of age. Mice at 4 months of age subjected to forced treadmill exercise at 15 m/min for 120 min were also analyzed for comparison (Ex (+), $n = 4$). **(E)** RT-qPCR analysis of PGC-1α isoform mRNAs in gastrocnemius of WT and KO mice as in (A) ($n = 6$). All quantitative data are means ± s.e.m. for the indicated numbers (n) of mice. $^{*}P < 0.05$, $^{**}P < 0.01$, and NS by two-way ANOVA with Bonferroni's post hoc test. **(F)** Model for the roles of PGC-1α isoforms in skeletal muscle. Circle sizes indicate the relative abundance of PGC-1α isoforms.

PGC-1α plays a key role in BAT thermogenesis [12,13,38]. We have now shown that PGC-1αb and PGC-1αc are also the major isoforms of PGC-1α induced in BAT by cold exposure. The upregulation of *Ucp1* in BAT and the maintenance of body temperature during cold exposure were thus impaired in PGC-1αAE1KO mice. Given that thermogenesis in BAT is coupled to the regulation of fat mass, it is possible that the obesity-prone phenotype of PGC-1αAE1KO mice is attributable in part to the impaired function of BAT.

Other than PGC-1αb and PGC-1αc, at least three other isoforms of PGC-1α (PGC-1α2, PGC-1α3, and PGC-1α4) are transcribed from AE1 [18]. However, in contrast to PGC-1αb and PGC-1αc, forced expression of these short isoforms in cultured myotubes did not induce the expression of genes related to energy metabolism, suggesting that loss of these isoforms likely does not contribute to the metabolic phenotypes of PGC-1αAE1KO mice. Transgenic overexpression of PGC-1α4 in skeletal muscle was previously shown to result in upregulation of skeletal muscle mass, suggesting that this isoform contributes to muscle hypertrophy [18]. In our study, PGC-1α4 also did not stimulate the transactivation activity of PPARα, nor did it interact with this transcription factor in cells. Moreover, PGC-1α4 did not affect mitochondrial respiratory function or proton leak, whereas the other three isoforms (PGC-1αa, PGC-1αb, and PGC-1αc) similarly promoted both. These observations are consistent with the findings of Ruas et al. They also showed that transgenic mice overexpressing PGC-1α4 manifested increased oxygen consumption and a reduced fat tissue mass. Given that PGC-1α4 did not induce the expression of genes related to mitochondrial function or energy metabolism, it suggested that the increase in oxygen consumption and decrease in WAT mass in the transgenic mice were not directly attributable to an ability of PGC-1α4 to regulate energy metabolism but rather than reflected secondary changes induced by the increase in skeletal muscle [18]. We found that skeletal muscle mass was unaltered in PGC-1αAE1KO mice (which lack PGC-1α4). It is therefore possible that PGC-1α4 is not required for the maintenance of skeletal muscle mass under the static condition, whereas it may contribute to the regulation of such muscle mass under other conditions.

PGC-1a has two different promoters that respond to two different stimuli, The β2-adrenergic agonist stimulated PGC-1αb/c promoter activity, whereas PGC-1αa promoter activity was not affected. The functional differences between the canonical PGC-1a (PGC-1αa) and the alternative PGC-1αb/c are due to differences in the regulation of gene expression. In several experiments, we have shown in vitro that the three PGC-1α isoforms (PGC-1αa, PGC-1αb, and PGC-1αc) have similar molecular functions. In addition, analysis of PGC-1αAE1KO mice showed that the adaptive induction of alternative variants of PGC-1α is important for metabolic adaptation to external stimuli. Our results provide insight into the differential physiological functions of PGC-1α isoforms in skeletal muscle (Figure 7F). Under the static condition, PGC-1α (predominantly PGC-1αa) plays an important role in skeletal muscle development by maintaining fiber-type composition, vascularity, and the amount of mitochondria [12–14,39]. In addition, PGC-1αa appears to be the major contributor to muscle remodeling in response to chronic exercise training. In contrast, PGC-1αb and PGC-1αc are largely responsible for the rapid induction of PGC-1α in skeletal muscle by acute exercise, with this effect being closely related to metabolic adaptation of skeletal muscle. The differential effects of exercise on the induction of PGC-1αa and PGC-1αb/c are, at least, partly, attributable to the different response of their promoters to β2-adrenergic stimuli. Moreover, PGC-1αAE1KO mice were unable to tolerate a heavy exercise load, suggesting that metabolic adaptation through exercise-induced PGC-1α expression is important for motor performance. As the expression of PGC-1α is also abundant in the heart, it is possible that reduced cardiac metabolism in PGC-1αAE1KO mice may also contribute to the reduced energy expenditure during exercise and exercise capacity.

PGC-1α is thought to be involved in the regulation of body mass and insulin sensitivity, but the previously reported metabolic phenotypes of PGC-1α-deficient mice have been inconsistent. Our findings suggest that the induction of PGC-1α that adapts to external stimuli, rather than its abundance under the static condition, plays an important role in the control of energy expenditure and fat mass by providing insight into the promoter of alternative variants of PGC-1α. Exercise mimetics are potential pharmacological treatments for obesity and T2D. A drug that can induce PGC-1αb/c independently of exercise, or one that can further enhance the expression of PGC-1αb/c during exercise, may potentially be developed as an exercise mimetic drug.

CREDIT AUTHORSHIP CONTRIBUTION STATEMENT

Kazuhiro Nomura: Writing — review & editing, Writing — original draft, Validation, Project administration, Methodology, Investigation, Funding acquisition, Formal analysis, Data curation, Conceptualization. **Shinichi Kinoshita:** Resources, Investigation. **Nao Mizusaki:** Investigation, Data curation. **Yoko Senga:** Investigation. **Tsutomu Sasaki:** Investigation. **Tadahiro Kitamura:** Investigation. **Hiroshi Sakaue:** Investigation. **Aki Emi:** Investigation. **Tetsuya Hosooka:** Investigation. **Masahiro Matsuo:** Investigation. **Hitoshi Okamura:** Investigation. **Taku Amo:** Investigation. **Alexander M. Wolf:** Investigation. **Naomi Kamimura:** Investigation. **Shigeo Ohta:** Investigation. **Tomoo Itoh:** Investigation. **Yoshitake Hayashi:** Investigation. **Hiroshi Kiyonari:** Resources. **Anna Krook:** Writing — review & editing, Supervision, Investigation. **Juleen R. Zierath:** Writing — review & editing, Supervision, Investigation. **Masato Kasuga:** Writing — review & editing, Supervision, Conceptualization. **Wataru Ogawa:** Writing — review & editing, Writing — original draft, Supervision, Project administration, Conceptualization.

ACKNOWLEDGMENTS

This work was supported by grants from the Ministry of Education, Culture, Sports, Science, and Technology of Japan to K.N. [Grant-in-Aid for Scientific Research C (26461337)], and to W.O. [Grant-in-Aid for Scientific Research on Innovative Areas (16H01391) and Grant-in-Aid for Scientific Research B (15H04848)]. We are grateful to Kyoko Toitani and Tomoya Kitazumi for technical assistance.

DECLARATION OF COMPETING INTEREST

The authors declare that they have no known competing financial interests or personal relationships that could have appeared to influence the work reported in this paper.

DATA AVAILABILITY

Data will be made available on request.

APPENDIX A. SUPPLEMENTARY DATA

Supplementary data to this article can be found online at https://doi.org/10.1016/j.molmet.2024.101968.

REFERENCES

[1] Handschin C, Spiegelman BM. Peroxisome proliferator-activated receptor γ coactivator 1 coactivators, energy homeostasis, and metabolism. Endocr Rev 2006;27(7):728–35. https://doi.org/10.1210/er.2006-0037.

[2] Pagel-Langenickel I, Bao J, Pang L, Sack MN. The role of mitochondria in the pathophysiology of skeletal muscle insulin resistance. Endocr Rev 2010;31(1):25–51. https://doi.org/10.1210/er.2009-0003.

[3] Mootha VK, Lindgren CM, Eriksson K-F, Subramanian A, Sihag S, Lehar J, et al. PGC-1α-responsive genes involved in oxidative phosphorylation are coordinately downregulated in human diabetes. Nat Genet 2003;34(3):267–73. https://doi.org/10.1038/ng1180.

[4] Patti ME, Butte AJ, Crunkhorn S, Cusi K, Berria R, Kashyap S, et al. Coordinated reduction of genes of oxidative metabolism in humans with insulin resistance and diabetes: potential role of *PGC1* and *NRF1*. Proc Natl Acad Sci U S A 2003;100(14):8466–71. https://doi.org/10.1073/pnas.1032913100.

[5] Kristensen JM, Skov V, Petersson SJ, Ørtenblad N, Wojtaszewski JørgenFP, Beck-Nielsen H, et al. A PGC-1α- and muscle fibre type-related decrease in markers of mitochondrial oxidative metabolism in skeletal muscle of humans with inherited insulin resistance. Diabetologia 2014;57(5):1006–15. https://doi.org/10.1007/s00125-014-3187-y.

[6] Skov V, Glintborg D, Knudsen S, Jensen T, Kruse TA, Tan Q, et al. Reduced expression of nuclear-encoded genes involved in mitochondrial oxidative metabolism in skeletal muscle of insulin-resistant women with polycystic ovary syndrome. Diabetes 2007;56(9):2349–55. https://doi.org/10.2337/db07-0275.

[7] Liang H, Balas B, Tantiwong P, Dube J, Goodpaster BH, O'Doherty RM, et al. Whole body overexpression of PGC-1α has opposite effects on hepatic and muscle insulin sensitivity. Am J Physiol Endocrinol Metab 2009;296(4):E945–54. https://doi.org/10.1152/ajpendo.90292.2008.

[8] Benton CR, Holloway GP, Han X-X, Yoshida Y, Snook LA, Lally J, et al. Increased levels of peroxisome proliferator-activated receptor gamma, coactivator 1 alpha (PGC-1α) improve lipid utilisation, insulin signalling and glucose transport in skeletal muscle of lean and insulin-resistant obese Zucker rats. Diabetologia 2010;53(9):2008–19. https://doi.org/10.1007/s00125-010-1773-1.

[9] Calvo JA, Daniels TG, Wang X, Paul A, Lin J, Spiegelman BM, et al. Muscle-specific expression of PPARγ coactivator-1α improves exercise performance and increases peak oxygen uptake. J Appl Physiol 2008;104(5):1304–12. https://doi.org/10.1152/japplphysiol.01231.2007.

[10] Choi CS, Befroy DE, Codella R, Kim S, Reznick RM, Hwang Y-J, et al. Paradoxical effects of increased expression of PGC-1α on muscle mitochondrial function and insulin-stimulated muscle glucose metabolism. Proc Natl Acad Sci U S A 2008;105(50):19926–31.

[11] Wong KE, Mikus CR, Slentz DH, Seiler SE, DeBalsi KL, Ilkayeva OR, et al. Muscle-specific overexpression of PGC-1a does not augment metabolic improvements in response to exercise and caloric restriction. Diabetes 2015;64:1532–43.

[12] Lin J, Wu P-H, Tarr PT, Lindenberg KS, St-Pierre J, Zhang C, et al. Defects in adaptive energy metabolism with CNS-linked hyperactivity in PGC-1α null mice. Cell 2004;119:121–35.

[13] Leone TC, Lehman JJ, Finck BN, Schaeffer PJ, Wende AR, Boudina S, et al. PGC-1α deficiency causes multi-system energy metabolic derangements: muscle dysfunction, abnormal weight control and hepatic steatosis. PLoS Biol 2005;3(4):e101. https://doi.org/10.1371/journal.pbio.0030101.

[14] Handschin C, Choi CS, Chin S, Kim S, Kawamori D, Kurpad AJ, et al. Abnormal glucose homeostasis in skeletal muscle–specific PGC-1α knockout mice reveals skeletal muscle–pancreatic β cell crosstalk. J Clin Investig 2007;117(11):3463–74. https://doi.org/10.1172/JCI31785.

[15] Kleiner S, Mepani RJ, Laznik D, Ye L, Jurczak MJ, Jornayvaz FR, et al. Development of insulin resistance in mice lacking PGC-1α in adipose tissues. Proc Natl Acad Sci U S A 2012;109(24):9635–40. https://doi.org/10.1073/pnas.1207287109.

[16] Miura S, Kai Y, Kamei Y, Ezaki O. Isoform-specific increases in murine skeletal muscle peroxisome proliferator-activated receptor-γ coactivator-1α (PGC-1α) mRNA in response to β2-adrenergic receptor activation and exercise. Endocrinology 2008;149(9):4527–33. https://doi.org/10.1210/en.2008-0466.

[17] Yoshioka T, Inagaki K, Noguchi T, Sakai M, Ogawa W, Hosooka T, et al. Identification and characterization of an alternative promoter of the human PGC-1α gene. Biochem Biophys Res Commun 2009;381(4):537–43. https://doi.org/10.1016/j.bbrc.2009.02.077.

[18] Ruas JL, White JP, Rao RR, Kleiner S, Brannan KT, Harrison BC, et al. A PGC-1α isoform induced by resistance training regulates skeletal muscle hypertrophy. Cell 2012;151(6):1319–31. https://doi.org/10.1016/j.cell.2012.10.050.

[19] Tadaishi M, Miura S, Kai Y, Kano Y, Oishi Y, Ezaki O. Skeletal muscle-specific expression of PGC-1α-b, an exercise-responsive isoform, increases exercise capacity and peak oxygen uptake. PLoS One 2011;6(12):e28290. https://doi.org/10.1371/journal.pone.0028290.

[20] Martínez-Redondo V, Pettersson AT, Ruas JL. The hitchhiker's guide to PGC-1α isoform structure and biological functions. Diabetologia 2015;58(9):1969–77. https://doi.org/10.1007/s00125-015-3671-z.

[21] Léveillé M, Besse-Patin A, Jouvet N, Gunes A, Sczelecki S, Jeromson S, et al. PGC-1α isoforms coordinate to balance hepatic metabolism and apoptosis in inflammatory environments. Mol Metab 2020;34:72–84. https://doi.org/10.1016/j.molmet.2020.01.004.

[22] Chan MC, Arany Z. The many roles of PGC-1α in muscle — recent developments. Metabolism 2014;63(4):441–51. https://doi.org/10.1016/j.metabol.2014.01.006.

[23] Jannig PR, Dumesic PA, Spiegelman BM, Ruas JL. SnapShot: regulation and biology of PGC-1α. Cell 2022;185(8). https://doi.org/10.1016/j.cell.2022.03.027. 1444–1444.e1.

[24] Yagi T, Tokunaga T, Furuta Y, Nada S, Yoshida M, Tsukada T, et al. A novel ES cell line, TT2, with high germline-differentiating potency. Anal Biochem 1993;214(1):70–6. https://doi.org/10.1006/abio.1993.1458.

[25] Inoue H, Ogawa W, Ozaki M, Haga S, Matsumoto M, Furukawa K, et al. Role of STAT-3 in regulation of hepatic gluconeogenic genes and carbohydrate metabolism in vivo. Nat Med 2004;10(2):168–74. https://doi.org/10.1038/nm980.

[26] Dong B, Hiasa M, Higa Y, Ohnishi Y, Endo I, Kondo T, et al. Osteoblast/osteocyte-derived interleukin-11 regulates osteogenesis and systemic adipogenesis. Nat Commun 2022;13(1):7194. https://doi.org/10.1038/s41467-022-34869-3.

[27] Ferrannini E. The theoretical bases of indirect calorimetry: a review. Metabolism 1988;37(3):287–301. https://doi.org/10.1016/0026-0495(88)90110-2.

[28] Severinsen MCK, Schéele C, Pedersen BK. Exercise and browning of white adipose tissue – a translational perspective. Curr Opin Pharmacol 2020;52:18–24. https://doi.org/10.1016/j.coph.2020.04.004.

[29] Ringholm S, Grunnet Knudsen J, Leick L, Lundgaard A, Munk Nielsen M, Pilegaard H. PGC-1α is required for exercise- and exercise training-induced UCP1 up-regulation in mouse white adipose tissue. PLoS One 2013;8(5):e64123. https://doi.org/10.1371/journal.pone.0064123.

[30] Fisher FM, Kleiner S, Douris N, Fox EC, Mepani RJ, Verdeguer F, et al. FGF21 regulates PGC-1α and browning of white adipose tissues in adaptive thermogenesis. Genes Dev 2012;26(3):271–81. https://doi.org/10.1101/gad.177857.111.

[31] Chinsomboon J, Ruas J, Gupta RK, Thom R, Shoag J, Rowe GC, et al. The transcriptional coactivator PGC-1α mediates exercise-induced angiogenesis in skeletal muscle. Proc Natl Acad Sci U S A 2009;106(50):21401–6. https://doi.org/10.1073/pnas.0909131106.

[32] Bézaire V, Seifert EL, Harper M. Uncoupling protein-3: clues in an ongoing mitochondrial mystery. FASEB J 2007;21(2):312–24. https://doi.org/10.1096/fj.06-6966rev.

[33] Clapham JC, Arch JRS, Chapman H, Haynes A, Lister C, Moore GBT, et al. Mice overexpressing human uncoupling protein-3 in skeletal muscle are hyperphagic and lean. Nature 2000;406(6794):415–8. https://doi.org/10.1038/35019082.

[34] Son C, Hosoda K, Ishihara K, Bevilacqua L, Masuzaki H, Fushiki T, et al. Reduction of diet-induced obesity in transgenic mice overexpressing uncoupling protein 3 in skeletal muscle. Diabetologia 2004;47(1):47–54. https://doi.org/10.1007/s00125-003-1272-8.

[35] Costford SR, Chaudhry SN, Crawford SA, Salkhordeh M, Harper M-E. Long-term high-fat feeding induces greater fat storage in mice lacking UCP3. Am J Physiol Endocrinol Metab 2008;295(5):E1018–24. https://doi.org/10.1152/ajpendo.00779.2007.

[36] Gong D-W, Monemdjou S, Gavrilova O, Leon LR, Marcus-Samuels B, Chou CJ, et al. Lack of obesity and normal response to fasting and thyroid hormone in mice lacking uncoupling protein-3. J Biol Chem 2000;275(21):16251–7. https://doi.org/10.1074/jbc.M910177199.

[37] Vidal-Puig AJ, Grujic D, Zhang C-Y, Hagen T, Boss O, Ido Y, et al. Energy metabolism in uncoupling protein 3 gene knockout mice. J Biol Chem 2000;275(21):16258–66. https://doi.org/10.1074/jbc.M910179199.

[38] Puigserver P, Spiegelman BM. Peroxisome proliferator-activated receptor-γ coactivator 1α (PGC-1α): transcriptional coactivator and metabolic regulator. Endocr Rev 2003;24(1):78–90. https://doi.org/10.1210/er.2002-0012.

[39] Lin J, Wu H, Tarr PT, Zhang C-Y, Wu Z, Boss O, et al. Transcriptional co-activator PGC-1α drives the formation of slow-twitch muscle fibres. Nature 2002;418(6899):797–801. https://doi.org/10.1038/nature00904.

